Testing the strength of thin glass

Francisco Esteves de Oliveira Santos
Instituto Superior Técnico, 2016

Abstract: Structural applications of glass are becoming increasingly more common, diverse and bold. Thin glass is a recent glass category, currently widespread in mobile devices and with great potential for applications in buildings, due to its remarkable developments in strength, flexibility and dimensions available. However, there is neither a standard method able to determine its strength nor experimental data available on its mechanical behaviour. In this context, experimental and numerical investigations were developed with two main goals: (i) to design or adapt setups to efficiently test the strength of thin glass and propose a new standard test to be used in structural design, and (ii) to characterize thin glass by using those tests, focusing on the ultimate strength and on particular behavioural aspects each test reveals more clearly. For this purpose, a set of non-destructive and destructive tests was carried out and a new test was proposed. Two non-destructive tests were investigated: the tin side detector test and the scattered light polariscope test. Concerning the first test, the equipment applied was found to be unsuitable for this kind of glass. The second test indicated much lower surface stresses than those reported by the producers of the thin glasses tested and those measured in the destructive tests. For destructive testing, another two tests were designed and assessed: the in-plane four-point bending test and the buckling test. While the first was prone to many geometrical instabilities, the second was able to cause failure of thin glass specimens, providing results for its strength, namely a lower bound imposed by the setup of 394 MPa (characteristic value) and 485 MPa (average value). In fact, the actual glass strength is expected to be significantly larger. Finally, based on the difficulties encountered in the destructive tests performed, a tension test was proposed and numerically investigated, revealing many potential advantages compared to the former in terms of quality of results and possibility of standardization.

Keywords: thin glass; strength; non-destructive testing; destructive testing; numerical modelling.

1. Introduction

Thin glass, or ultra-light glass, usually refers to glasses with thickness below 2 mm (Albus & Robanus, 2015), particularly in the range of 0,55 to 2,00 mm (Neugebauer, 2015). In terms of composition, thin glass can be made of soda-lime glass, borosilicate glass or aluminosilicate glass. Usually, these glasses are produced using either the micro-float, the down-draw or the overflow-fusion processes and then are tempered through thermal or chemical processes to enhance the mechanical properties. Thin glass presents a combination of high strength and thinness that results in a flexible material with a wide range of applications. Usually, thin glass refers to aluminosilicate chemically tempered glass as it presents the most interesting properties.

There is a broad range of industries where thin glass has potential to be applied. In civil engineering, thin glass could be used: (i) as a flat panel, such as in tensile façades or overhead glazing with long spans, where its high strength is a significant advantage and self-weight would be an issue; (ii) as a cold-bent panel, such as in any curved design or membrane structures replacing the expensive process of bending glass; or (iii) in adaptive or dynamic designs, making use of its flexibility in uses such as moveable elements, e.g., stadium roofs or canopies, or adaptive façades. However, prior to any of those structural applications, it is required to determine its strength.

Presently, major producers of thin glass, such as Corning, SCHOTT or AGC, report compressive stresses up to 900 MPa. As most current applications of thin glass (such as mobile devices) are not necessarily dependent on the value of its strength, specific testing of thin glass revolves around impact behaviour, surface hardness, flexibility and only seldom on its strength, generally determined in small samples, so the values attained would suffer from considerable size effects if extrapolated to the civil engineering scale.

Considering the standard methods to test the strength of glass, namely the EN ISO 1288, it is clear that the geometrical nonlinearities thwart the correct procedure and calculations of the strength of thin glass. In fact, the relevant tests that this norm comprises are two coaxial double ring tests and a four-point bending test; while the first is used for applications where the edge is not loaded, the latter also stresses the edge. One important note is that both tests assume small deformations and the Bernoulli theory, so the deformations are limited up to a percentage of the thickness. The norm also describes the parameters that influence the strength tests: surface condition, rate and duration of loading, area of surface loaded in tension, ambient medium, age, and temperature. Finally, it states the conditions to perform the strength tests: temperature of 23 ± 5ºC, relative humidity between 40% and 70% and stress rate of 2 ± 0,4 MPa/s (EN ISO 1288, 2016).

A few recent studies focused on testing the strength of thin glass, namely those of Siebert (2013), Spitzhüttl *et al*. (2014), Maniatis *et al*. (2014) and Neugebauer (2016). In a first phase, these studies focused on the standard tests of EN ISO 1288, and then proposed alternatives. The next paragraphs summarize their findings about both the standard tests (double coaxial tests and four-point bending tests) and the alternatives, including the multiple point bending test and the buckling test.

The European Norm specifies two coaxial double ring tests: the EN ISO 1288-2, for larger applications, and the EN ISO 1288-5, for smaller ones. Even for the smaller samples, Neugebauer (2016) confirms the need to take into account geometrical nonlinearities (key factor), size effects and imperfections of the setup or glass plate. His experimental and numerical tests revealed large asymmetric deformations, as depicted in Figure 1. Stresses were no longer uniform on the stressed area.

Figure 1 – Coaxial double ring test R105 (Neugebauer, 2016)

For the four-point bending test, described in EN ISO 1288-3, the deformations are simply too large (Figure 2). Maniatis *et al.* (2014) proposed using the same dimensions for the setup but with a modified analytical approach to include the geometrical nonlinearities, such as the horizontal reaction forces developed at the supports. In this study, experiments were also conducted in fully tempered thin glass samples. However, this setup becomes impracticable for higher strength values or lower thicknesses: considering a 2 mm thick chemically tempered glass plate with a strength of 600 MPa to 800 MPa, the ultimate curvature radius would be between 90 mm and 120 mm; for smaller thicknesses, it would even be lower. The plate would simply slip between the supports before being broken.

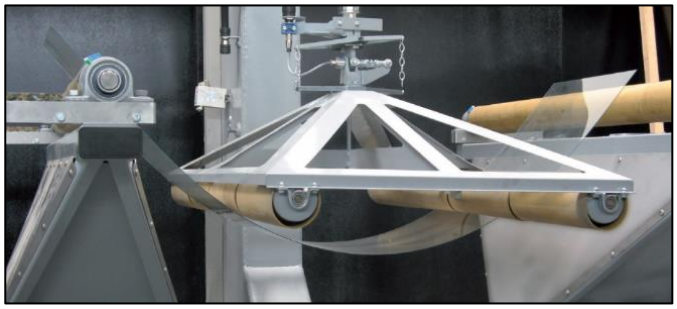

Figure 2 – Four-point bending test in 2,00 mm thin glass with strength of 120 MPa (Holzinger, 2011)

A modification to this setup was proposed by Siebert (2013) and Neugebauer (2016), the multiple-point bending test, which consists of several pairs of loads and supports in order to introduce maximum stresses on a considerable length, but distributed over several smaller loading spans (Figure 3). One of the main drivers for this setup is the possibility to use the standard 1100 x 360 mm^2 plates. Nonetheless, the setup was never validated experimentally and presents many difficulties, such as its sensitivity to imperfections in the setup geometry.

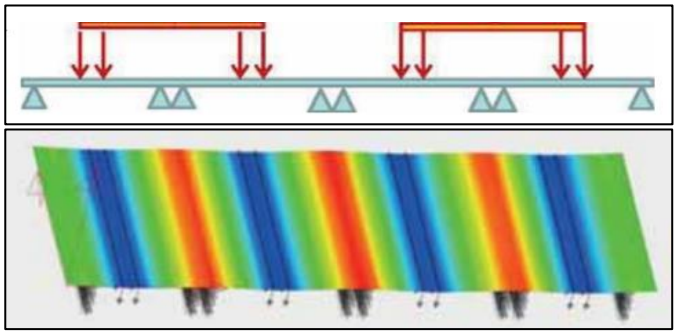

Figure 3 – Illustrative scheme of the setup and of the stresses developed on the top surface (Siebert, 2013)

Finally, another test presented in all the above-mentioned four articles is the buckling test. In this case, the glass panel is supported vertically by two rollers that rotate around the weak axis of inertia of the plate and is loaded by an in-plane force on the top; the force causes the buckling and an increasing out-of-plane deflection. Spitzhüttl *et al.* (2014) and Maniatis *et al.* (2014) carried out experimental investigations on fully tempered thin glass plates with dimensions of 1100x360 mm^2. The maximum vertical displacement attained was 75 mm, corresponding to a strength/stress of around 125 MPa. The vertical displacement *vs*. axial stress curves obtained for different specimens were not consistent and, more importantly, it was not possible to determine an estimate for the tensile strength. Finally, these experiments were complemented with numerical studies to provide further insights on the stress distribution (Figure 4) and to assess the influence of the Young's modulus, the thickness and the Poisson's ratio.

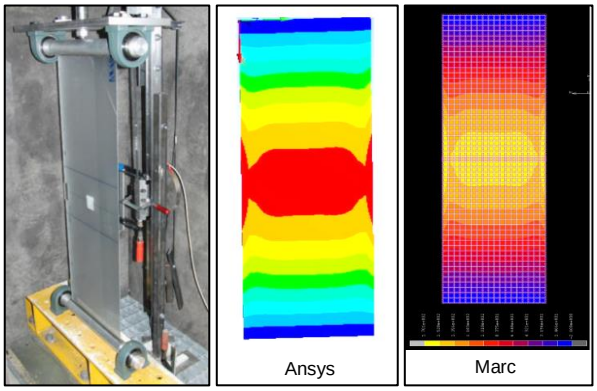

Figure 4 - Buckling test setup and plot of the distribution of the main stresses with two FE software (Spitzhüttl et al., 2014)

The literature review shows that a new standard for testing the strength of thin glass is required in order to trigger the use of thin glass as a structural element. Hence, new methods of testing must be designed and tested thoroughly to come up with a valid solution that offers coherent and insightful results through a standardisable methodology.

Consequently, this experimental and numerical study was developed with two main goals: (i) to design or adapt setups to efficiently test the strength of thin glass and propose a new standard test to be used in structural design, and (ii) to characterize thin glass by using those different tests, focusing on the ultimate strength and on the particular behavioural aspect each test reveals more clearly.

For this purpose, a set of tests was planned: as non-destructive tests, the tin side detector test and the Scattered Light Polariscope (SCALP) test were assessed; and as destructive tests, the in-plane four-point bending test and the buckling test were analysed. After conducting the tests, analysing and discussing the results obtained, a new method was designed and proposed.

The experimental program is based on samples of Leoflex glass, produced by AGC. It is an aluminosilicate chemically tempered glass with compressive stresses in the range of 600 MPa to 800 MPa, as reported by the producer. The samples used were plates with a thickness of 2 mm, height of 80 mm and length of 710 mm. For the analyses carried out, the relevant properties are as follows: Young's modulus, E=74 GPa; shear modulus, G=30 GPa, Poisson's ratio v = 0,233; photoelastic constant, C=28,3 nm/cm.MPa and refraction index, RI=1,508. Complementary to these samples, other materials were employed to study certain aspects and are referred in the non-destructive or destructive tests, according to their use.

2. Non-destructive testing

Non-destructive techniques are a much more cost-efficient way of testing as the specimen remains unaltered after the exam, which is particularly important in the case of thin glass, because specimens with adequate dimensions are still very expensive. In the case of the experiments performed, the tin side detector test and the SCALP test consist in emitting UV light and a laser beam, respectively, in the specimen being tested.

As a complementary material, smaller specimens of a similar thin glass by another producer, SCHOTT's Xensation thin glass, was available in 5 different thicknesses (0,55; 0,70; 1,10; 2,00 and 3,00 mm), with the following relevant properties: refractive index of 1,514 at the compressive layer and of 1,506 in the core, and photoelastic constant of 29,2 nm/cm.MPa.

2.1. Tin side detector test

In the float or micro-float production processes, the side of the glass in contact with the molten tin is usually known as the "tin side". After being removed, traces of tin or tin oxide deposited during the cooling stage can be found on this surface of glass. The other side is identified as "air side".

The goal of this test is to verify if the tin side is still detectable after the ion exchange. As there is evidence that the tin might hinder the exchange of ions in the chemical temper (Jiang *et al.,* 2012), this is particularly important for studying the glass strength, despite this test not providing an ultimate value for this parameter. If indeed the tin was detectable, that influence would then be studied with the SCALP test.

The tin side detector used was the model *TS1301* produced by *C.R. Laurence Co., Inc.*, without any digital capabilities. The tests were carried out in: a 2,00 mm thick sample of thin glass (AGC Leoflex); small samples of various thicknesses (0,55; 0,70; 1,10; 2,00 and 3,00 mm; SCHOTT Xensation); and a sample of 10 mm thick float glass. All the glass samples were produced with float or micro-float processes. The test was performed in a dark room.

The first method used was the *"bottom side method" or "through glass testing".* The detector is placed on the side of the glass and one observes if either the laser or a blur is visible from the opposite side of the glass (Figure 5). On the thick float glass it was clearly distinguishable one side that glowed more and made the UV light blurry (tin side) and other side where the lamp was clearly visible, with little to no distortion (air side). However, in all the thin glass samples, it was impossible to notice any significant difference. The glass seemed slightly translucent with the same intensity for each of its sides and due to its thinness, it was not possible to verify if one of the sides was glowing more.

The other method used, the *"top side method"*, consists in placing the detector on the top edge of the glass, tilting the glass and irradiating its side surface - if there is a glow, it corresponds to the tin side (Figure 6). It is more focused on the surfaces and the influence of the glass thickness is decreased. As expected, this method provided good results for the thick float glass. However, it also failed to provide convincing or clear results for the thin glass samples, as both sides were sort of translucent.

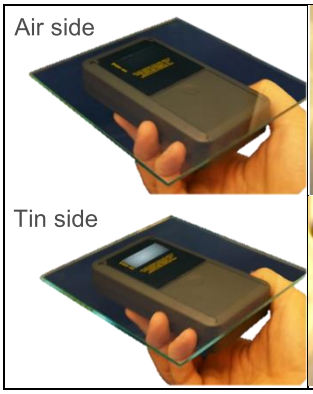

Figure 5 – "Bottom side" testing (C.R.Laurence Co.,Inc.)

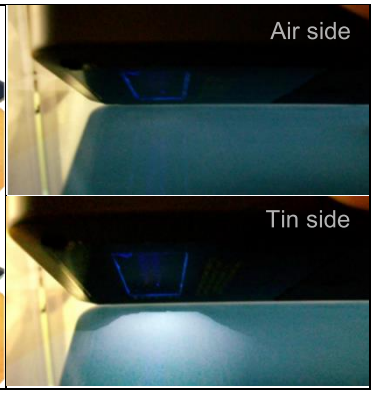

Figure 6 – "Top side" testing (C.R.Laurence Co.,Inc.)

2.2. Scattered Light Polariscope test

The main goal of the SCALP test is to obtain the value of the stress at the surface of a glass plate and to study the stress distribution both along the area of the plate and as a function of the depth; it is also used to study the influence of the tin side.

The test principle is based on the concepts of stress birefringence and photoelasticity of glass. Birefringence is a phenomenon in which a ray of light passing through a given material experiences two refractive indices. Photoelasticity is a property of materials that exhibit birefringence when subjected to stresses. Several methods use this property to gain insights on the distribution of stresses in glass, of which five stand out: frozen stress method, integrated photoelasticity, photoelastic tomography, mirage method and scattered light method (Aben *et al*., 2008).

The method chosen for the analysis was the scattered light method. The device used was the *Scattered Light Polariscope 05* (SCALP-05) equipment manufactured by *GlasStress*. It emits a 5 mW polarized laser beam with a wavelength of 635 nm (GlasStress Ltd, 2013). Figure 7 illustrates the test principle. The beam passes through the polariscope prism and enters the glass panel at a specific angle. As it passes through the panel, the laser is scattered in planes perpendicular to the beam. The polarization of the scattered laser changes due to the stress birefringence. Variation of the polarization also means variation of the intensity. Those changes are recorded by a charge coupled device (CCD) camera that has a high quality sensor in terms of accuracy and light sensitivity. The laser beam is optically modulated and light intensities recorded by the camera from each pixel should vary sinusoidally. The variation of the intensity of the scattered light along the laser beam is registered, the retardation through the panel thickness processed and fitted into a retardation curve (retardation fit) and, finally, that curve is inverted and the stress profile is calculated.

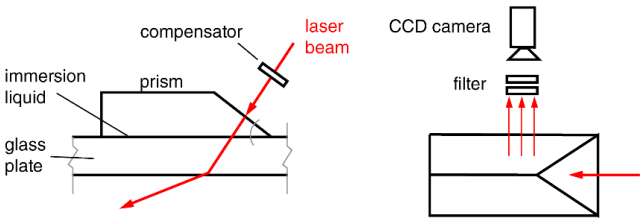

Figure 7 – Side and top view of the SCALP working principle (adapted from Aben et al., 2008)

Current research on thermally tempered glass found a good correlation between compressive stress and strength, therefore proposes to reconsider the standard four-point bending test (EN ISO 1288-3) and fragmentation test (EN 12150-1), both destructive and expensive, in favour of these residual stress measurements (Aben *et al*., 2010).

For this research, the methodology followed in the tests is described in the manual of SCALP (GlasStress Ltd, 2013). Some adaptations were made to understand the influence of particular parameters in the results and an extensive set of preliminary tests was carried out.

Of all the readings performed, and taking into account the objective of this analysis, three tests were selected as they fulfil different and complimentary goals. These tests are the following: (i) the full-length test (ii) the area test and (iii) the test with different thicknesses. The goals of these tests are summarized in Figure 8.

Name of analysis	Full-length test	Area test	Test with different thicknesses
Goal	Understand the distribution of the residual stress along the total length of the plate	Investigate the surface stress near the ends and corners of the plate and the symmetry of the stress distribution	Study the stress profile of different thicknesses and of samples produced by different manufacturers
Readings	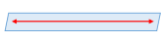	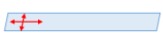	

Figure 8 – The three SCALP tests carried out – summary of goals and focus of the readings done

i. Full length test

The full-length test consisted of consecutive readings spaced of 10 mm along the whole length of the plate. The polariscope was positioned in the centre of the plate's width and moved to the following position by slowly sliding it aided by ruled paper used as a background. At the 24th centimetre, the polariscope was removed and cleaned, hence the results presented in Figure 9 are divided in "before" and "after" (cleaning).

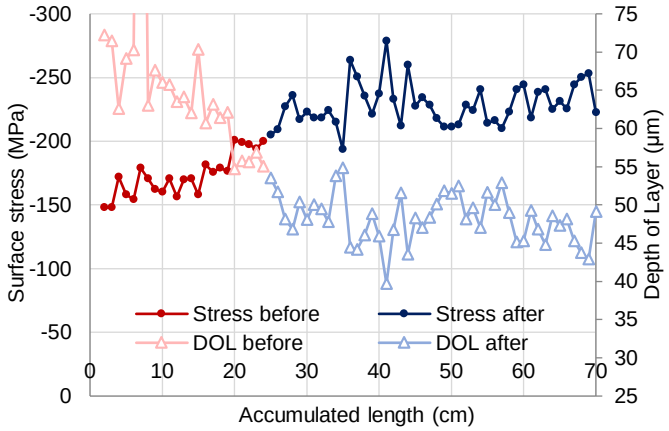

Figure 9 – Surface stress and depth of layer along the whole length of the plate

The following main conclusions can be drawn: there is a strong negative correlation between surface stress and depth of layer (DOL), which is suggested in AGC's product datasheet; the magnitude of the obtained surface stresses is far below the value of 800 MPa, expected for the type of glass being tested.

ii. Area test

The aim of the area test was to study the surface stress distribution on the area, particularly near the edges and corners. Six positions were chosen to make the measurements, with the SCALP pointing for two or three directions in each reading point, as illustrated in Figure 10 with the respective results. A significant symmetry was observable in the stress measurements; however, the magnitude of the surface stresses was far below than what was expected.

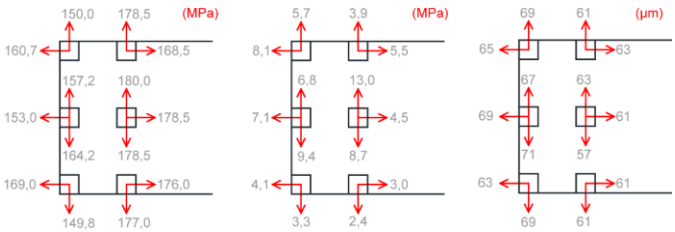

Figure 10 – Scheme of the stress results (MPa) with respective standard deviations and DOL (µm) for the area test

iii. Test with different thicknesses

For this test, five different samples of glass from SCHOTT were used with thicknesses of 0,55, 0,70, 1,10, 2,00 and 3,00 mm. Results are presented in Table 1. One did not expect the specimens' thickness to have significant influence on the results provided by the SCALP tests, since the compressive layer should have similar depth for the different specimens tested; however, such influence is visible on the surface stress values and on the standard deviation ones. For a thickness of 1,10 mm, a positive surface stress (*i.e.*, tensile) was determined, without any apparent explanation.

Table 1 – Results of SCALP readings for SCHOTT Xensation samples with 5 different thicknesses

Sample thickness (mm)	#meas.	Surface Stress (MPa)	St. Deviation (MPa)	Meas. Depth (mm)	Depth of layer (µm)	Fit error (MPa)
0,55	50	-107,7	54,6	0,55	113,8	4,9
0,70	25	-168,8	121,7	0,70	126,7	3,5
1,10	50	+586,1	23,9	1,10	52,3	3,6
2,00	50	-616,1	3,8	2,00	111,1	3,1
3,00	50	-170,8	12,1	3,00	111,7	4,9

3. Destructive testing

In destructive testing, experiments are carried out up to failure, in order to investigate the specimens' performance or the material behaviour when subjected to mechanical loads. These tests generally yield more information and are easier to interpret than non-destructive tests, as they can replicate more closely the effects of actual loading conditions.

For both tests conducted herein, a stress rate of 2 ± 0,4 MPa/s was applied, following the EN ISO 1288 specifications.

As a complementary material, samples of aluminium of the same dimensions of the Leoflex glass plates were employed, making use of a similar Young's modulus to study the test setup and prevent flaws that would compromise samples of (more expensive) thin glass.

3.1. In-plane four-point bending test

The main goal of this test is to investigate the ultimate strength of a thin glass sample, knowing that the most tensioned part of the section is the edge. As the thin section is subjected to in-plane loads applied at the top edge, lateral buckling is likely to occur. Therefore, to determine the ultimate strength of glass, it is of interest to prevent such instability.

The advantages of this test method are the following: the four-point bending setup has been thoroughly studied for many applications; it focuses strictly on the edge over a significant length and is the best setup to study the strength of such component; furthermore, if well designed, the behaviour of the sample is linear, not requiring much instrumentation to obtain the results. The difficulties lie on the effective lateral constraint and on the concentration of stresses on the points of contact between glass and metallic parts of the setup.

The test setup is a four-point bending configuration, with 600 mm between supports and 200 mm between loads (Figure 11).

The lateral constraint used in this test is composed of two 15 mm thick aluminium plates and their final dimensions were 710 mm by 80 mm, just like the glass plate (Figure 12). Between these plates and the test specimen, stripes of Teflon are glued to reduce the drag and a rubber band is placed at supports and load points.

Three versions of the setup, with a gradual increase of the stiffness of the lateral constraint, were tested, mostly on aluminium samples and on one thin glass sample. The tests are

extensively described in (Santos, 2016). In summary, the main features and modifications of the setups were as follows:

1. Continuous lateral constraint leaving some free height at the bottom and top of the glass; outer supports only - AL1, AL2;
2. Increase of the height of the lateral constraint to cover the whole glass surface; introduction of rubber bands - AL3, AL4
3. Introduction of two very stiff inner supports; different connections of the machine to the cross-head – AL5, AL7, AL8, GLASS.

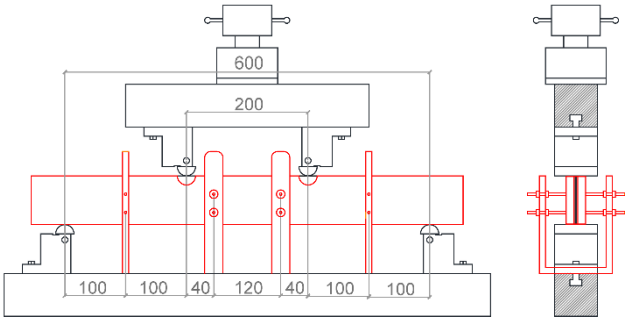

Figure 11 – In-plane four-point bending final setup, front and side view, with focus on dimensions and lateral constraint (red)

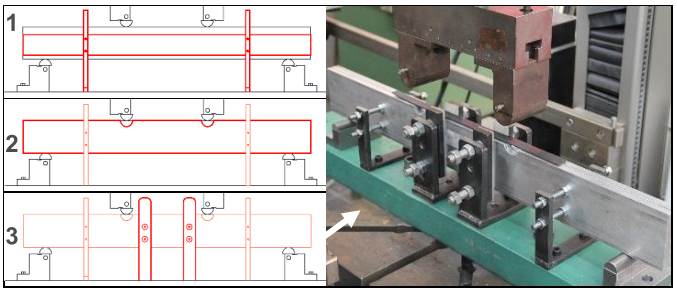

Figure 12 – Iterations of the lateral constraint of the setup

The results are presented in Figure 13 by sets of colours: yellow for the first version; green for the second, blue for the third and red for glass. It is clear that the behaviour is far from linear, and although the stiffness of the lateral constraint allows to reach higher values of stress, there are many nonlinearities involved.

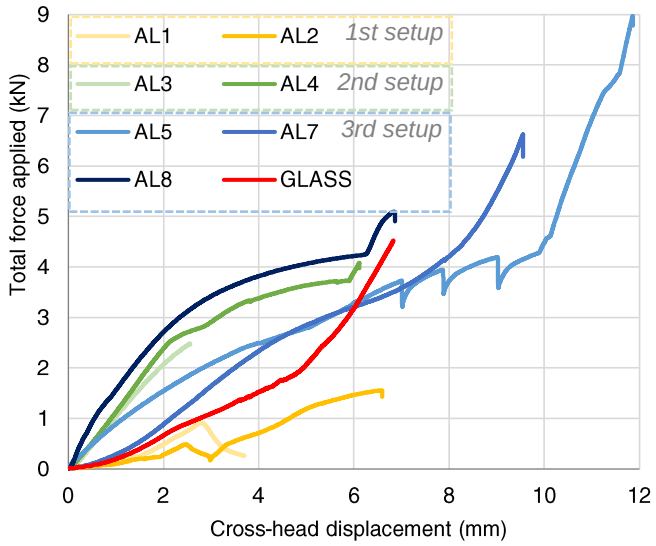

Figure 13 – Force-displacement graph for all preliminary tests

Besides the nonlinear behaviour, the failure of the glass sample seems to have been caused by a flaw on the edge of the glass (Figure 14), so no conclusions were drawn regarding strength. A final version of the setup was proposed, but it was decided to save the samples of thin glass to the buckling tests.

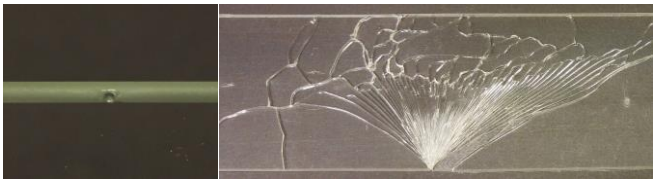

Figure 14 – Detail of a flaw on the edge of the sample tested and corresponding cracking pattern

A numerical analysis was planned and executed with two objectives: to study the behaviour of samples without lateral instability and strictly under bending and to investigate the lateral torsional buckling behaviour. Therefore, Santos (2016) presents numerical finite element models of the various experimental setups used to test aluminium and glass panes, including an analysis on the instability; herein only the analyses with glass are presented and are summarized in Figure 11.

Name	Analysis 1	Validation	Analysis 2	Analysis 3
Goal	Understand the theoretically perfect behaviour of the test, with no lateral displacement	Validate the new model, its geometry and elements used (with many more dof)	Study the lateral torsional buckling phenomenon and the influence of the lateral supports	Study the lateral torsional buckling phenomenon and the influence of the lateral supports
Setup	Perfectly constrained	1st and 2nd setups	1st and 2nd setups	3rd setup
dof	Two: $\{u_x, u_y\}$	Five: $\{u_x, u_y, u_z, \phi_x, \phi_y\}$	Five: $\{u_x, u_y, u_z, \phi_x, \phi_y\}$	Five: $\{u_x, u_y, u_z, \phi_x, \phi_y\}$
Lateral constr.	Perfectly constrained	Only outer supports	Only outer supports	Outer and inner sup.
Lateral force	No lateral / horizontal force applied	No lateral / horizontal force applied	Horiz. forces applied proportionally to verti. displacement at loads	Horiz. forces applied proportionally to verti. displacement at loads

Figure 15 – In-plane four-point bending setup, front and side view,

The results are shown in Figure 16 and Figure 17. The linear analysis confirmed that the maximum stress is mostly located on the edge and this stress distribution is identical to all samples prior to buckling. Concerning the lateral instability analyses, it was shown that the setup is prone to buckling and once it occurs, the stress distribution varies widely along the surface of the glass, making it impossible to assess the ultimate strength.

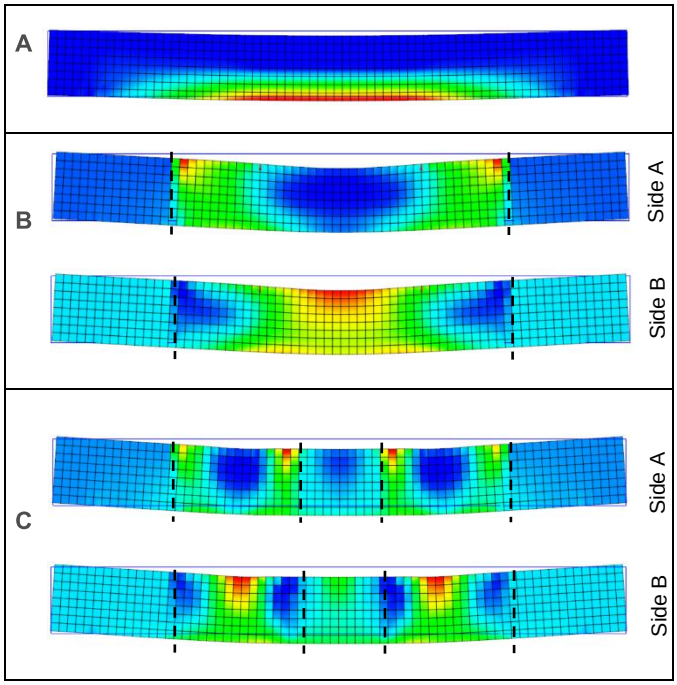

Figure 16 – Stress distribution at 12 mm of vertical displacement, for analyses 1, 2 and 3 and indication of lateral supports

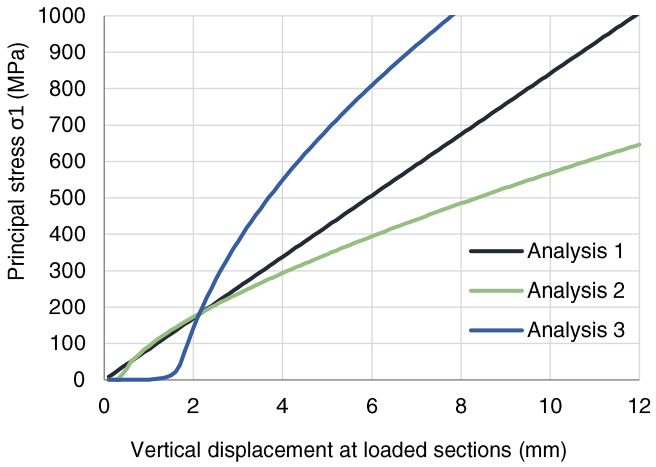

Figure 17 – Principal stress at critical points vs. vertical displacement at loaded sections for all three analyses

3.2. Buckling test

The high potential of application of curved or flexible glass plates of large dimensions motivates the interest in studying their buckling behaviour, besides the assessment of the ultimate strength of the material.

One of the advantages of this buckling test is the introduction of the maximum stress over a considerable area, in a way that is very similar to realistic applications. It allows assessing the performance of thin glass plates in terms of flexibility and curvature.

The buckling test setup, illustrated in Figure 18, consisted of a glass plate supported at the top and bottom edges by a cylindrical roller that constrained rotations around all axes but the weakest axis of inertia of the plate. The rollers used in the setup have 25 mm of radius and contain a 7 mm deep slit, who could not be deeper due to technical reasons. It is important to mention that the slit has a width of 2,5 mm, so it allowed some movements of the glass plate; a preliminary test with a 2,0 mm wide slit revealed problems in the removal of the shatters of the glass after breakage and was thus altered.

The test itself consisted of applying a vertical displacement on the top roller; when a sufficient vertical load was applied, a horizontal displacement was manually and momentarily imposed to set the direction of buckling towards the intended side (protected by an acrylic box).

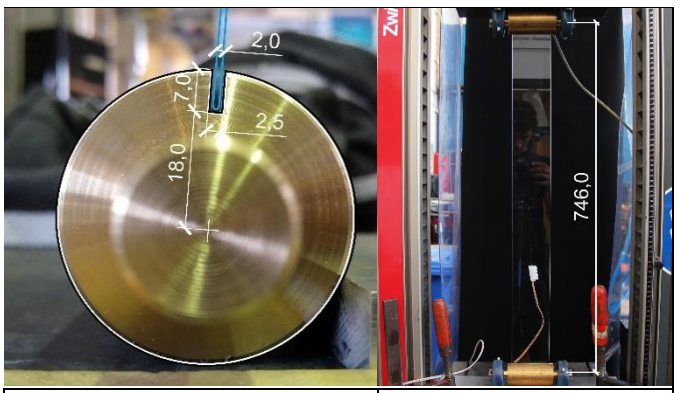

Roller - side view	*Setup - front view*

Figure 18 – Pictures of the test setup with dimensions (mm)

To measure the axial strains, the vertical relative displacement (between rollers) and the corresponding vertical force, the instrumentation consisted of the load cell and displacement transducer of the compression machine (*Zwick 010*), strain gauges and cameras. The out-of-plane deformation (z-axis) was not measured. However, some solutions were studied: the use of laser sensors; the use of wire LVDTs (horizontally positioned at the beginning of the tests) and the triangulation of their results; and a camera recording a side-view with a ruled background.

A numerical analysis was also performed, with the main goal of simulating the experimental tests presented above and to obtain a better understanding of the behaviour of the tested plates. In fact, comparing numerical and experimental results allows drawing further conclusions to the behaviour observed in the experiments, provides more information.

Figure 19 illustrates the model of the glass plate. Curved shell quadrilateral finite elements with 10 mm of width were chosen and the basic geometry set was a continuous element of 746x80x2 mm^3. In terms of loads, an initial (horizontal) deformation (1 mm) was introduced by applying a point load in the z-direction at the centre of the plate, thus inducing the consequent buckling, which was then caused by an in-plane displacement (in the x-direction) applied at the top end. The boundary conditions are illustrated in Figure 19.

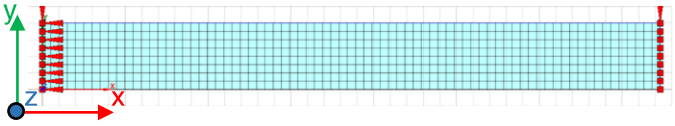

Figure 19 – Geometry, mesh and boundary conditions for the buckling model

A detailed description of both the preliminary tests and of the instrumentation, as well as of the numerical model (including the loading process, the finite elements used and a study of the initial imperfection) is presented in Santos (2016).

In the following paragraphs, the results of the experimental tests on 10 samples (plus one outlier) and of the numerical analysis are compared and discussed. This discussion of the results starts with the analysis on the applied force, followed by the analysis of the stress. Two analyses of the stress distribution are presented: a vertical and a horizontal profile of the stresses. Finally, the fracture and strength of thin glass is analysed.

Concerning the applied force, the experimental data was obtained with the compression machine and showed a remarkable coherency in terms of behaviour. The numerical model presents slight differences of behaviour comparing with the experimental results, particularly regarding the triggering of the instability (Figure 20). For both experimental and numerical data, buckling starts at around the same applied force, but while experimental results reveal an increase of force and then a sudden drop with the buckling, the numerical results initially present a lower force with a much smoother increase of deformation. Then, the behaviour stabilizes and the curves become almost parallel, with an offset of around 5,5 N to 6,5 N. It is noteworthy to mention that the overall behaviour reflected by the experimental and numerical curves is consistent with the (expected) stable buckling behaviour of an elastic material.

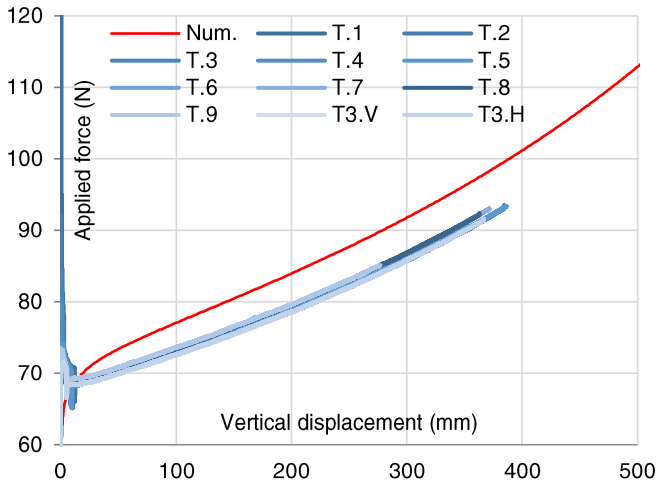

Figure 20 – Applied force vs. vertical displacement, comparison of numerical and experimental values

In terms of axial stress, the strain was experimentally measured with a strain gauge at the centre of the glass plates, and then converted to stress by applying the Hooke's Law, with E=74,0 GPa. The numerical behaviour seems remarkably close to the experimental results, as presented in Figure 21. However, a more detailed analysis shows that the stress ratio between numerical and experimental tests starts at around 1,35 and slowly converges to around 1,17.

It is worth mentioning that the displacement rate used (2,085 mm/s) proved to correspond to the intended stress rate of 2,0 MPa/s. In the first stage of the test, a much higher stress rate occurred, but from an axial stress of 200 MPa up to the failure of the samples the planned stress rate was kept roughly constant (Santos, 2016).

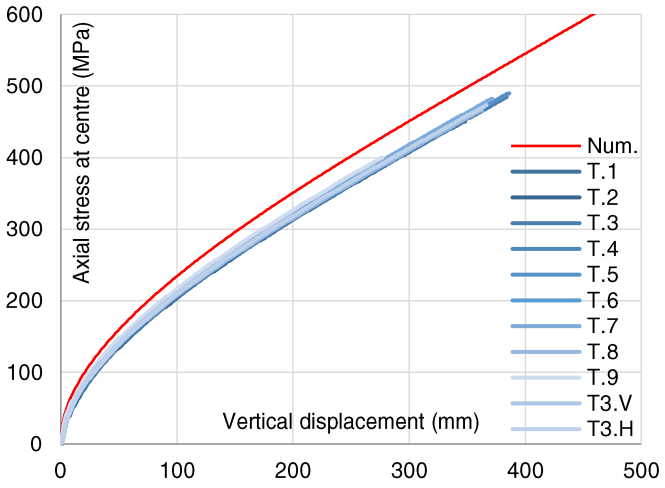

Figure 21 – Stress at centre of outer surface vs. vertical displacement, comparison with experimental values

To obtain the stress profile, one of the thin glass samples (T3.V) was instrumented with three strain gauges: one at the centre (A) (as all the others presented in Figure 21) and the two other below the central one at distances of 100 mm (B) and 200 mm (C). For each type of analysis, experimental and numerical, Figure 22 illustrates the stress ratio between the stress at the centre (A) and at the remaining locations. Consequently, the relative values *A' Num.* and *A* are always 1,00.

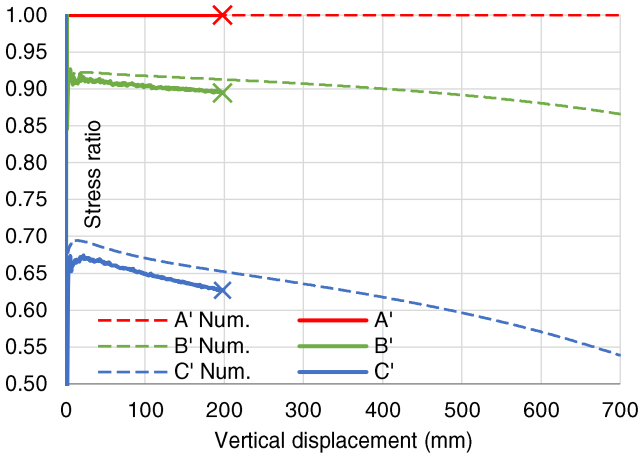

Figure 22 – Numerical and experimental vertical distribution of stress vs. vertical displacement; comparison and ratio (T3.V)

Figure 23 presents the results of a similar analysis, which focused on the horizontal profile of axial stresses. With that purpose, one of the thin glass samples was instrumented with three strain gauges at mid-height: two near the edge of the plate, but still in the plane surface (A and C), and one at the centre (A), as all the others presented in Figure 21. The overall behaviour of experimental and numerical curves is also quite similar, revealing that the stresses at the edges are 1,18 to 1,09 times higher than at the centre. For the width of the section, the experimental to numerical ratio is almost identical, even for such a detailed scale as the one presented in the plot.

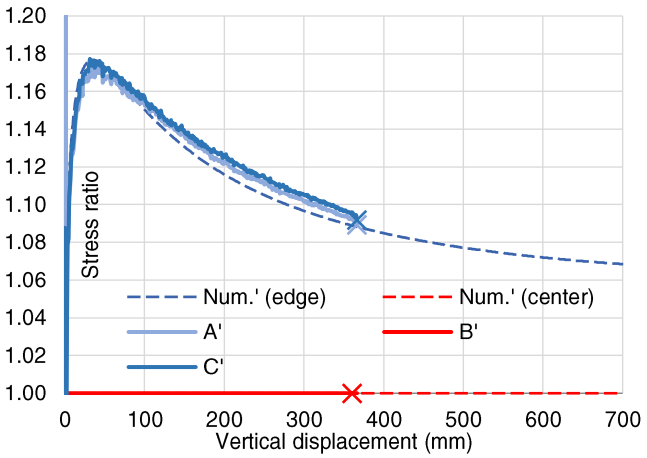

Figure 23 – Numerical and experimental horizontal distribution of axial stress vs. vertical displacement; comparison and ratio (T3.H)

In spite of the above-mentioned success in terms of coherency and consistency of experimental results, the plate was not fully clamped in the rollers' slits. In fact, this factor had some influence in the experimental behaviour, which justifies the differences to the numerical results. In Figure 24, the problem becomes clear: the glass-metal contact is located on very thin lines and the centre of the roller is not aligned with the axis of the plate. These factors make the plate more unstable and promote the buckling triggering at a lower load, causing the out-of-plane deformation to reduce as the plate finds a way to display a less stressed configuration, therefore lowering the stresses for the same applied load. To sum up, the transition from glass to metal done by the slit, which was neglected in the numerical analysis, causes the stress distribution to behave as

if the lengths of the numerical and experimental tests were different.

Moreover, and more importantly than simple behavioural aspects, the ultimate strength/collapse seems to have been caused precisely by the contact of the glass plate with the rollers, as attested by video frames and by a geometrical analysis of the supports area. The glass/metal contact is located on very thin lines and there is not any auxiliary material to distribute the tension stresses that are developed, so the maximum stress attained is likely limited by the setup.

Figure 24 also illustrates a proposed alternative setup, including a neoprene band, which provides the following potential advantages: (i) the lower elastic modulus of neoprene provides a much better (more uniform) stress distribution; (ii) the applied loads are rather low so the resulting stress and deformations at the neoprene will be negligible; (iii) the behaviour is close to clamped and allows removing the glass shatters after the collapse; (iv) the centre of the roller is coincident with the end of the glass plate, making the height of the setup the same as the height of the plate; (v) finally, it has the advantage of increasing the range of thicknesses possible to test, being enough to couple the glass thickness with an appropriate thickness of the neoprene band. To conclude, the proposed geometry seems to offer many benefits over the former setup, mainly leading to a design compliant with standard sizes and providing a much closer agreement with the theoretical behaviour expected for well-defined boundary conditions; it is an upgraded version of the one that was used in the tests and could stand as a standard test.

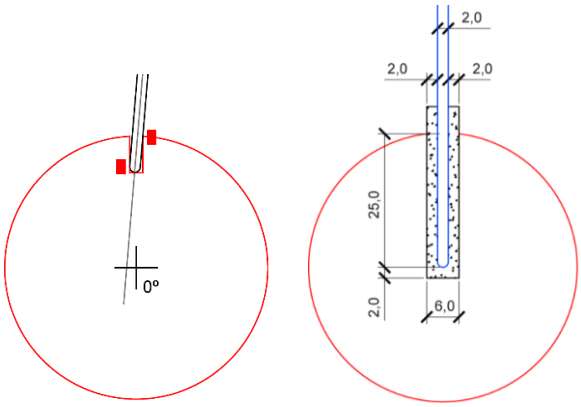

Figure 24 – Contact areas (red) between glass and metallic roller and proposed setup

Concerning the analysis of the collapse, Figure 25 plots the ultimate stresses obtained at the centre of the plate. The average ultimate strength obtained in the centre strain gauge of the 10 samples considered is $\bar{x}$ = 444,7 MPa, with a standard deviation of σ = 50,2 MPa (coefficient of variation of 11,3%). The maximum stess value is 489,6 MPa and the minimum one is 318,2 MPa, with 7/10 samples presenting maximum stress above 450 MPa. Assuming a normal distribution, the characteristic value of the maximum stress is f_k = 362MPa.

Taking into consideration that the stress at the edges is 1,09 times higher than at the centre in the brink of collapse (T3.H sample broke at 473 MPa), those values could be multiplied by this coefficient to determine the ultimate stress on the material: hence, $\bar{x}_{max}$ = 485MPa and $f_{k;max}$ = 394 MPa.

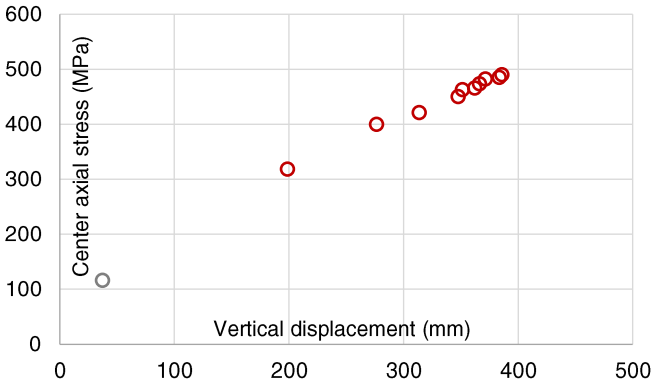

Figure 25 – Graphs of ultimate values of stress in function of the vertical displacement

To conclude, and despite having only 10 samples, a 2-parameter Weibull distribution was also used to describe the experimental results. The following parameters were obtained: σ_0 = 471,69 MPa and m = 7,89. A probability of 5% is achieved for a stress of $f_{k;5\%}$ = 325 MPa. The stress coefficient concerning the edge effect was not considered for this distribution, but if applied it would lead to a characteristic stress of $\sigma_{0;max}$ = 514 MPa. Once more, note that the stresses obtained in these analyses (regardless of the statistical distribution considered) are a lower bound of the actual tensile strength of the thin glass tested (as it was prematurely caused by the stress concentrations at the slits of the cylinders).

3.3. Brief reflection about the tests performed

The two tests setups developed and presented in the previous sections provided interesting insights on the behaviour of thin glass and on the procedures to test it. However, both tests presented problems regarding their application or standardization.

The four-point bending test is a rather complex test to perform correctly due to the high forces at stake and the very thin section that quickly becomes unstable, even with lateral constraints.

The buckling test was fairly easy to set as the geometrical nonlinearities are easily predictable and are even used as part of the test principle, leading to very consistent test results. However, the test principle is closely related to the minimum curvature radius of the glass plate, which depends on its thickness and on the ultimate strength of glass. Hence, very thin plates or the ever growing strength of glass pose considerable difficulties to the experimental determination of the ultimate strength of glass and might compromise the applicability of this type of test.

Therefore, an alternative testing method, the tension test, was designed. The goal of this test setup, presented in the next subsection, is to be able to be applied to any thickness and strength, and become the standard for the testing of thin glass. However, due to time limitations, it was not possible to assess this test, so no experimental results are shown, only results of numerical analyses.

3.4. Proposed test to study the strength: tension test

The main goal of the tension test is to study the behaviour of glass under pure tension and to determine its ultimate strength. It has the advantage of subjecting almost all the length of the plate to the maximum stress, with the particularity of not being prone to any kind of instability and nonlinearity. Therefore, it can be applied to any thickness, providing a measurement of the ultimate tensile strength.

The difficulties of the test proposed lie in this specimen being a uniform rectangle with the same section along the whole length; usually, specimens used for tensile tests have a dog-bone shape (with a thicker and broader part), so that even though there is load transfer from/to the test machine and stress concentrations may develop, this does not occur at the critical section. However, that type of section is not possible to implement in the (thin) glass samples. Therefore, a glued connection is proposed.

The setup consists of two pairs of metallic plates that are glued with a proper adhesive to both sides of the glass plate, a pair for each extremity of the plate. The metallic plates assure the connection of the glass specimen to the tensile machine; this connection is done through a steel cylinder inserted in a hole of the same radius in the metallic plates (Figure 26).

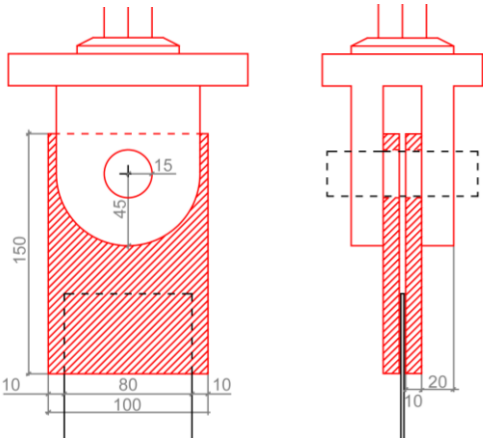

Figure 26 – Tension test setup, front and side view

The numerical analysis had the main goal of predicting the behaviour of the glued connection and the distribution of stresses in the different materials.

The glass was modelled as a linear material with elastic and shear moduli of 74 GPa and 30 GPa respectively. A commercially available glue (Ultra Light-Weld® 431 by DYMAX) was selected and deemed as appropriate, being modelled as a nonlinear elasto-plastic material with a von Mises yield stress of 23 MPa and an elastic modulus of 574 MPa. Neither the Poisson's ratio nor the shear modulus were provided by the manufacturer, but the study by Nhamoinesu & Overend (2012) on similar glass-steel adhesives reported a range of values for the Poisson's ratio (ν) from 0,29 to 0,48. Therefore, these two Poisson's ratios were used to study its impact on the behaviour of the test and cover the whole range expected for this material property. Herein, more focus is given to the lowest value, as it was found to provide better results.

From the analysis of the applied force *vs*. the displacement at the outer surface of the glue, illustrated in Figure 27, it is evident that the Poisson's ratio is not relevant for the applied force. Six points covering the linear and yielding phases of the adhesive are highlighted and used later in this section to illustrate the analyses of the stress distribution.

The analysis of the stresses developed in the glass surface was carried out by plotting the values of the principal stress σ1 on the centre (C) and on the edge (E) for the six points presented in Figure 27 over a profile of 80 mm starting from the top of the glass plate and for ν = 0,29 (Figure 28). The stresses reach 800 MPa and are quite homogeneous, without relevant peaks.

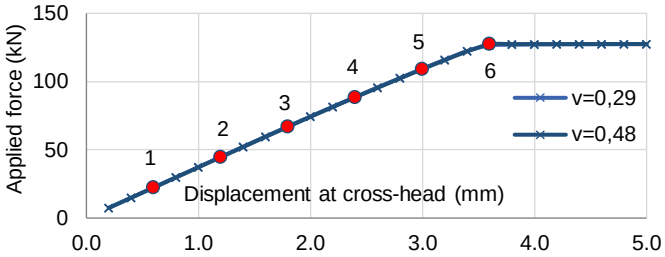

Figure 27 – Applied force vs. vertical displacement at the outer surface of the glue (half of cross-head displacement)

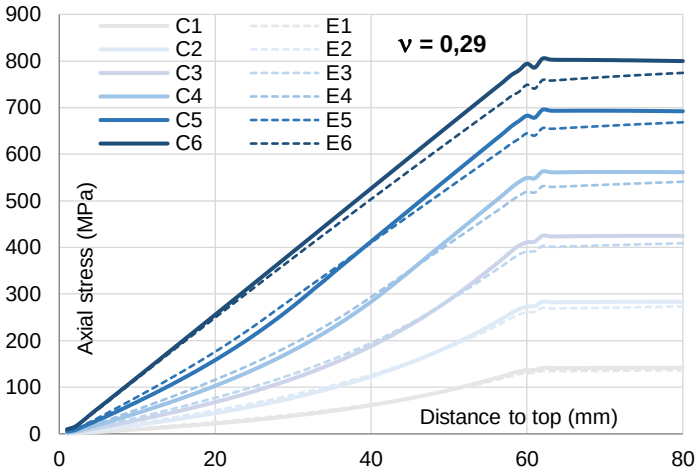

Figure 28 – Evolution of centre (C) and edge (E) axial stresses in the glass, vertical profile (ν = 0,29)

A similar analysis was carried out about the surface shear stress profile over the glued length (60 mm). For the referred six load values listed, the shear stresses at the centre and at the edge along the glued length were computed for ν = 0,29 (Figure 29). The yielding occurred for stresses of 13,3 MPa, which is in agreement with the von Mises yield stress set as input.

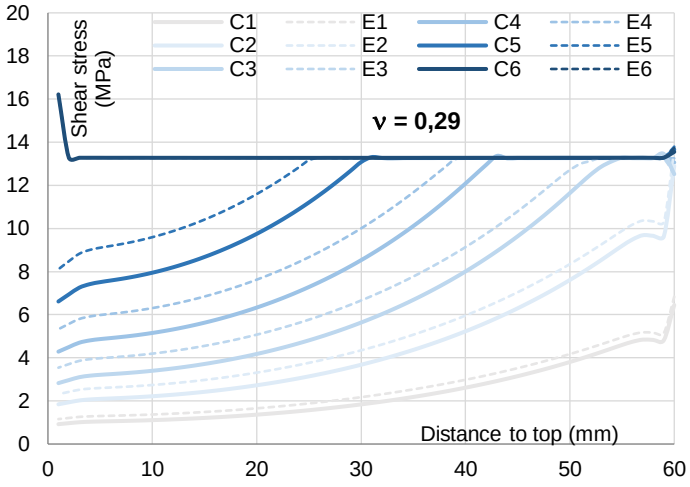

Figure 29 – Evolution of centre (C) and edge (E) shear stresses in the glue, vertical profile (ν = 0,29)

4. Conclusions

This section presents the main conclusions obtained in this study, including those from the non-destructive and destructive tests.

For the **tin side detector test**, the results obtained were inconclusive and indicate that the test is not appropriate for chemically tempered thin glass, at least with methodology and equipment used.

Regarding the **SCALP test**, a significant offset was found between the magnitudes of the values provided by the producers to the ultimate stress (from 600 MPa to 800 MPa), those obtained from the mechanical tests (around 450 MPa to 500 MPa[1]) and the results of the SCALP test (200 MPa). Still, it was confirmed that the DOL and the surface stress have a strong negative correlation.

The **four-point in-plane bending test** required a significant development of the setup, including several iterations to overcome the various difficulties that were encountered. Together with the numerical analyses, it is concluded that if thin glass is subjected to in-plane loading, lateral instability is a serious concern and it is not easy to prevent this phenomenon effectively. Furthermore, such instability deeply affects the stress distribution and renders impossible the attempts to determine the strength of thin glass.

Concerning the **buckling test**, the test principle is based on the geometrically nonlinear deformations developed in the specimen and the setup used indeed cause very significant deformations in the test specimens. The test provided very coherent and consistent experimental results in terms of applied forces and stresses, whose behaviour was well simulated in the numerical analysis. However, the tests were affected by the slit of the roller, which not only justifies the slight differences between the experimental and numerical analyses, but also seems to have caused the premature collapse of the specimens, due to the stress concentrations at the slits (in this test the shatters of the collapsed glass plates were very small, almost powder-like). Therefore, the maximum stress values attained are a lower bound of the strength of thin glass. As a consequence, a new setup was proposed to prevent such stress concentrations.

In spite of the above mentioned difficulties, the average maximum stress measured at the centre of the 10 samples was 445 MPa. These results provided 5% probabilistic values of $f_{k;Normal}$ = 362 MPa for a normal distribution, and $f_{k;Weibull}$ = 325 MPa for the 2-parameter Weibull distribution. In terms of stress distribution, the maximum stress developed at the edges of the plate at the mid-height section; when the sample collapsed, the stress at the edge (at mid-height) was 1,09 times higher than at the centre. If this factor is taken into account, the maximum stress at breakage has an average of 485 MPa and a characteristic value of 394 MPa or 514 MPa, for the normal and 2-parameter Weibull distributions, respectively. It is also worth mentioning that the maximum stress attained within the samples tested was 490 MPa (at the centre), which would translate in around 534 MPa at the edges (considering the coefficient of 1,09). Once more, these figures are a lower bound of the actual tensile strength.

Although some improvements were suggested to enable using this test setup, the applicability of the test principle is hardly compatible with very thin plates or the ever growing strength of glass. In this context, an alternative test was finally proposed, the **tension test**, which seems to be the one with the most potential in terms of application and standardization, provided that the issues concerned with the glued connection are dealt with correctly. The numerical study revealed that the nonlinearity and elongation of the glue suggested to be used to bond the glass plate to the metallic plates provides a very homogeneous load transfer from the glass being tested to the outer surface of the metallic plate of the test fixture. The main advantages of this test over the former two are the following: (i) the thickness or strength of the thin glass samples are less likely to compromise the collapse of the test specimen, as the curvature radius is not involved; (ii) the portion of the glass area subjected to the maximum stress compared with the total area is much higher; (iii) the test is dominated by a geometrically linear behaviour; and (iv) the yielding of the glue allows for a quite homogeneous load transfer, and although it introduces some nonlinearity in the force-displacement response, the stress develops linearly in most of the glass area.

[1] Strength values are a lower bound. As mentioned, there might have been an upper limit imposed by the setup of the test.

5. References

Aben, H., Anton, J., & Errapart, A. (2008). Modern Photo elasticity for Residual Stress. (B. P. Ltd, Ed.) *Strain 44*, 40-48.

Aben, H., Anton, J., Errapart, A., Hödemann, S., Kikas, J., Klaassen, H., & Lamp, M. (2010). On non-destructive residual stress measurement in glass panels. *Estonian Journal of Engineering*, 16, 150-156.

Albus, J., & Robanus, S. (2015). Glass in Architecture - Future developments. *Detail*.

EN 1288:2000 Glass in building - Determination of the bending strength of glass. Brussels: European Committee for Standardization (CEN).

GlasStress Ltd. (2013). *SCALP Instruction Manual Ver. 5.8.2.* GlasStress Ltd.

Holzinger, P. (2011). Thin glass technology for insulating glass production. *Glass Performance Days.* Finland: GPD.

Jiang, L., Guo, X., Li, X., Li, L., Zhang, G., & Yan, Y. (2012). Different K+–Na+ inter-diffusion kinetics between the air side and tin side of an ion-exchanged float aluminosilicate glass. *Applied Surface Science,* 265, 889-894.

Maniatis, I., Nehring, G., & Siebert, G. (2014). *Studies on determining the bending strength of thin glass.* ICE Publishing. *Structures and Buildings*, 169, 393-402.

Neugebauer, J. (2015). A Movable Canopy. *International Conference on Building Envelope Design and Technology.* Graz.

Neugebauer, J. (2016). Determining of Bending Tensile Strenght of Thin Glass. *Challenging Glass 5.* Ghent.

Nhamoinesu, S., & Overend, M. (2012). The Mechanical Performance of Adhesives for a Steel-Glass Composite Façade System. *Challenging Glass 3.* TU Delft: Challenging Glass 3.

Santos, F. O. (2016). *Testing the strenght of thin glass.* Master thesis. Lisbon: Instituto Superior Técnico.

Siebert, G. (2013). Thin glass elements - a challenge for new applications. *Glass Performance Days 2013*, (pp. 316-319). Tampere, Finland.

Spitzhüttl, J., Nehring, G., & Maniatis, I. (2014). Investigations on determining the bending strength of thin glass. *Challenging Glass 4 & COST Action TU0905 Final Conference* (pp. 521-530). Leiden: CRC Press/Balkema.